Neurobiology of Disease 130 (2019) 104493

Contents lists available at ScienceDirect

Neurobiology of Disease

journal homepage: www.elsevier.com/locate/ynbdi

Amyotrophic Lateral Sclerosis-associated GGGGCC repeat expansion promotes Tau phosphorylation and toxicity

Hua He[a,1], Wen Huang[a,1], Ruoxi Wang[a], Yunting Lin[a], Yichen Guo[a], Jing Deng[a], Haitao Deng[a], Yanping Zhu[a], Emily G. Allen[b], Peng Jin[b,*], Ranhui Duan[a,*]

[a] Center for Medical Genetics & Hunan Key Laboratory of Medical Genetics, School of Life Sciences, Central South University, Changsha, Hunan 410078, China
[b] Department of Human Genetics, School of Medicine, Emory University, Atlanta, GA, USA

ARTICLE INFO

Keywords:
Drosophila
C9ORF72
G_4C_2 repeat expansion
Tau
ALS

ABSTRACT

Microtubule-associated protein Tau (MAPT) and GGGGCC (G_4C_2) repeat expansion in chromosome 9 open reading frame 72 (*C9ORF72*) are the major known genetic causes of frontotemporal dementia (FTD) and other neurodegenerative diseases, such as Amyotrophic Lateral Sclerosis (ALS). Although expanded G_4C_2 repeats and Tau traditionally are associated with different clinical presentations, pathological and genetic studies have suggested a strong association between them. Here we demonstrate a strong genetic interaction between expanded G_4C_2 repeats and Tau. We found that co-expression of expanded G_4C_2 repeats and Tau could produce a synergistic deterioration of rough eyes, motor function, life span and neuromuscular junction morphological abnormalities in *Drosophila*. Mechanistically, compared with the normal allele containing $(G_4C_2)_3$ repeats, the $(G_4C_2)_{30}$ allele increased Tau phosphorylation levels and promoted Tau R406W aggregation. These results together suggest a potential crosstalk between expanded G_4C_2 repeats and Tau in modulating neurodegeneration.

1. Introduction

Neurodegenerative disorders can lead to cognitive deficits, as seen in Alzheimer's disease (AD) and frontotemporal dementia (FTD), but can also affect motor systems, as seen in Amyotrophic Lateral Sclerosis (ALS) and Parkinson's disease (PD) (Gan et al., 2018). The neuropathology associated with the presentation of FTD is frontotemporal lobar degeneration (FTLD), degeneration in the cortical and subcortical structures within the frontal and temporal lobes (Rademakers et al., 2012). The most common genetic cause of FTD and ALS is a G_4C_2 repeat expansion in the first intron of the *C9ORF72* gene (Renton et al., 2011; DeJesus-Hernandez et al., 2011). The expansion accounts for ~40% and ~25% of familial ALS and FTLD, respectively, and 6%–7% of sporadic ALS and FTD cases (Rademakers et al., 2012; Liu et al., 2014; Cooper-Knock et al., 2014).

The majority of FTLD cases are caused by intracellular aggregates of Tau or TDP-43, referred to as FTLD-Tau or FTLD-TDP, respectively (Elahi and Miller, 2017). Tau is a highly soluble microtubule-associated protein predominantly expressed in neurons, encoded by the microtubule-associated protein Tau (*MAPT*) gene. Tauopathies are characterized by the progressive accumulation of filamentous hyperphosphorylated Tau inclusions in patient brains. Tauopathy-related diseases include AD, FTD, progressive supranuclear palsy (PSP), corticobasal degeneration (CBD), agyrophilic grain disease (AGD), Pick disease (PiD), and Huntington disease (HD) (Spillantini and Goedert, 2013; Mann and Snowden, 2017). The primary function of Tau is to promote microtubule assembly and stabilization. Under pathologic conditions, Tau is hyperphosphorylated and impaired in its ability to bind and stabilize microtubules, thus promoting Tau self-assembly and aggregation (Wang and Mandelkow, 2016; Holtzman et al., 2016; Alonso and Cohen, 2018). Hyperphosphorylated Tau can aggregate into filaments, and these Tau filaments can continue to aggregate and form insoluble deposits, which are referred to as neurofibrillary tangles (NFTs) that are found in Tauopathy patients (Wang and Mandelkow, 2016; Holtzman et al., 2016; Alonso and Cohen, 2018). Research in AD cases showed that Tau is hyperphosphorylated in NFT development, causing the transition from pre-tangles to NFT formation (Kimura et al., 2018; Neddens et al., 2018). The immunostaining of postmortem brains with anti-phospho-Tau antibodies such as AT8 (pS199/pS202/pT205), AT180 (pT231), and AT270 (pT181) can be used as an indicator of pre-tangle Tau, thought to be an early event in NFT formation (Neddens et al., 2018; Kimura et al., 1996; Augustinack et al., 2002).

* Corresponding authors.
E-mail addresses: peng.jin@emory.edu (P. Jin), duanranhui@sklmg.edu.cn (R. Duan).
[1] [1]H. He and W. Huang contributed equally to this work.

https://doi.org/10.1016/j.nbd.2019.104493
Received 4 January 2019; Received in revised form 21 May 2019; Accepted 5 June 2019
Available online 06 June 2019
0969-9961/

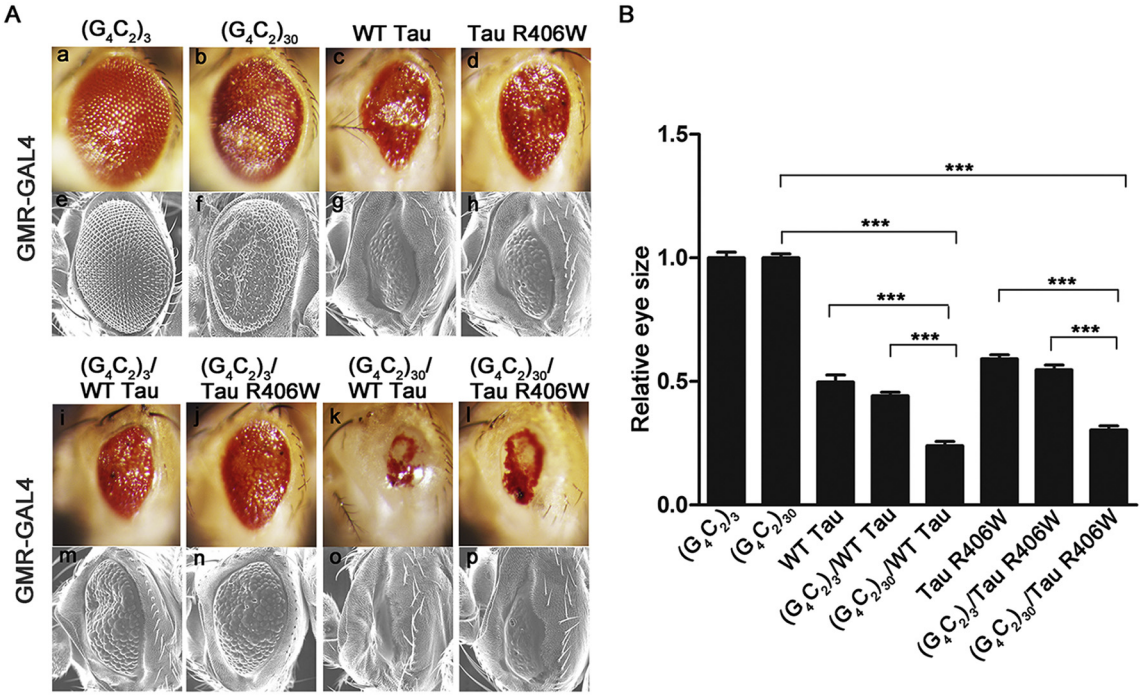

Fig. 1. Coexpression of G_4C_2 repeat and Tau enhances toxicity in Drosophila eyes.
A. Expression of the G_4C_2 repeat and Tau in the Drosophila eye by light (a-d, i-l) and scanning electron microscope (e-h, m-p). All flies are shown at 2 weeks after eclosion; (a, e) Gmr-GAL4 > $(G_4C_2)_3$; (b, f) Gmr-GAL4 > $(G_4C_2)_{30}$; (c, g) Gmr-GAL4 > Tau WT; (d, h) Gmr-GAL4 > Tau R406W; (i, m) Gmr-GAL4 > Tau WT + $(G_4C_2)_3$; (j, n) Gmr-GAL4 > Tau R406W + $(G_4C_2)_3$; (k, o) Gmr-GAL4 > Tau WT + $(G_4C_2)_{30}$; (l, p) Gmr-GAL4 > Tau R406W + $(G_4C_2)_{30}$;
B. Analysis of eye size of G_4C_2 and Tau flies. *** $p < 0.001$ after controlling for multiple testing using one-way ANOVA with the Tukey posthoc test.

Missense mutations in Tau were identified in inherited cases of FTD as early as 1998, revealing that Tau could be the primary cause of disease (Hutton et al., 1998; Spillantini et al., 1998; Poorkaj et al., 1998). However, the pathogenic role of the repeat expansion in *C9ORF72* wasn't discovered until 2011 (Renton et al., 2011; DeJesus-Hernandez et al., 2011). Since this discovery, researchers have worked to understand the clinical variation with the G_4C_2 repeat expansion. Studies have tried to identify potential genetic modifiers contributing to the phenotypic variability seen with *C9ORF72* repeat expansions. One study identified the co-occurrence of Tau mutation, p.P301L, in an FTLD patient with a *C9ORF72* expansion (van Blitterswijk et al., 2013). Another Tau variant, p.A239T, was found in a woman with behavioral variant FTLD with the *C9ORF72* mutation. This patient displayed a dominant neuropathology with Tau positive Pick bodies. As the p.A239T variant was not previously associated with Tau pathology, this study indicated that *C9ORF72* mutation appeared to be predominantly associated with the Tauopathy (King et al., 2013).

Pathological and genetic studies have suggested an association between G_4C_2 repeat expansion and Tauopathy. In addition to the discovery of various Tau mutations in patients with G_4C_2 expansions (van Blitterswijk et al., 2013; King et al., 2013), FTLD patients with only *C9ORF72* expansions have been found with Alzheimer-type pathology that is characterized by amyloid plaques and NFTs (Murray et al., 2011; Ferrari et al., 2012). Moreover, Tauopathy was systematically evaluated in a series of 17 FTLD cases with *C9ORF72* mutations (FTLD-*C9ORF72*), 13 cases of FTLD linked to progranulin mutations (FTLD-GRN), and 36 cases of sporadic FTLD (sFTLD). Significantly more NFTs and higher Tau burden were seen in FTLD-*C9ORF72* cases compared with FTLD-GRN cases, and a trend was seen for higher NFT stage compared with sporadic FTLD (Bieniek et al., 2013). These results suggest *C9ORF72* expansions might favor the aggregation and accumulation of Tau proteins.

Drosophila models have provided important insight for many forms of human neurodegenerative diseases (Chan and Bonini, 2000; Bonini and Fortini, 2003). The fly eye is used to study the pattern of neurodegeneration in these disorders. Alteration of the highly regular structure of the *Drosophila* retina provides an easily discernable phenotype for scoring neurodegeneration (Bonini and Fortini, 2003). In the current work, we use the *Drosophila* model to explore the association of G_4C_2 repeat expansion and Tau. We have previously shown that the presence of 30 G_4C_2 repeats in a *Drosophila* model was sufficient to cause neurodegeneration (Xu et al., 2013). In this work, we show that both wild type and mutant Tau (R406W) produced pathological synergistic deterioration with the G_4C_2 expansion, including reduced eye size, shortened lifespan, impaired movement ability, and abnormal neuromuscular junction (NMJ) morphology. Compared with $(G_4C_2)_3$ repeats, $(G_4C_2)_{30}$ increased Tau phosphorylation levels and promoted Tau R406W aggregation and increased CDK5 phosphorylation. Thus, our results suggest a genetic link between G_4C_2 repeat expansion and Tauopathy.

2. Methods

2.1. Fly stocks and genetics

Fly culture and crosses were performed on standard food according to standard procedures and raised at 25 °C. The GMR-GAL4 (no.8605) and elav-GAL4 (C155) were obtained from the Bloomington *Drosophila* Stock Center at Indiana University (Bloomington, IN, USA). UAS-$(G_4C_2)_{30}$-EGFP and UAS-$(G_4C_2)_3$-EGFP lines used in this study were described previsouly (Xu et al., 2013). The transgenic *Drosophila* lines expressing human wild-type and R406W mutant Tau were described previously (Wittmann et al., 2001). The expression of $(G_4C_2)_{30}$ in all cells of the peripheral and central nervous system using elav-GAL4 caused lethality in early development as described previously (Xu et al., 2013). As the pupal lethality of $(G_4C_2)_{30}$ precluded studies in mature neurons of the adult brain, we used *elav-Gal4* coupled with a ubiquitously expressed temperature-sensitive allele of the Gal80 repressor

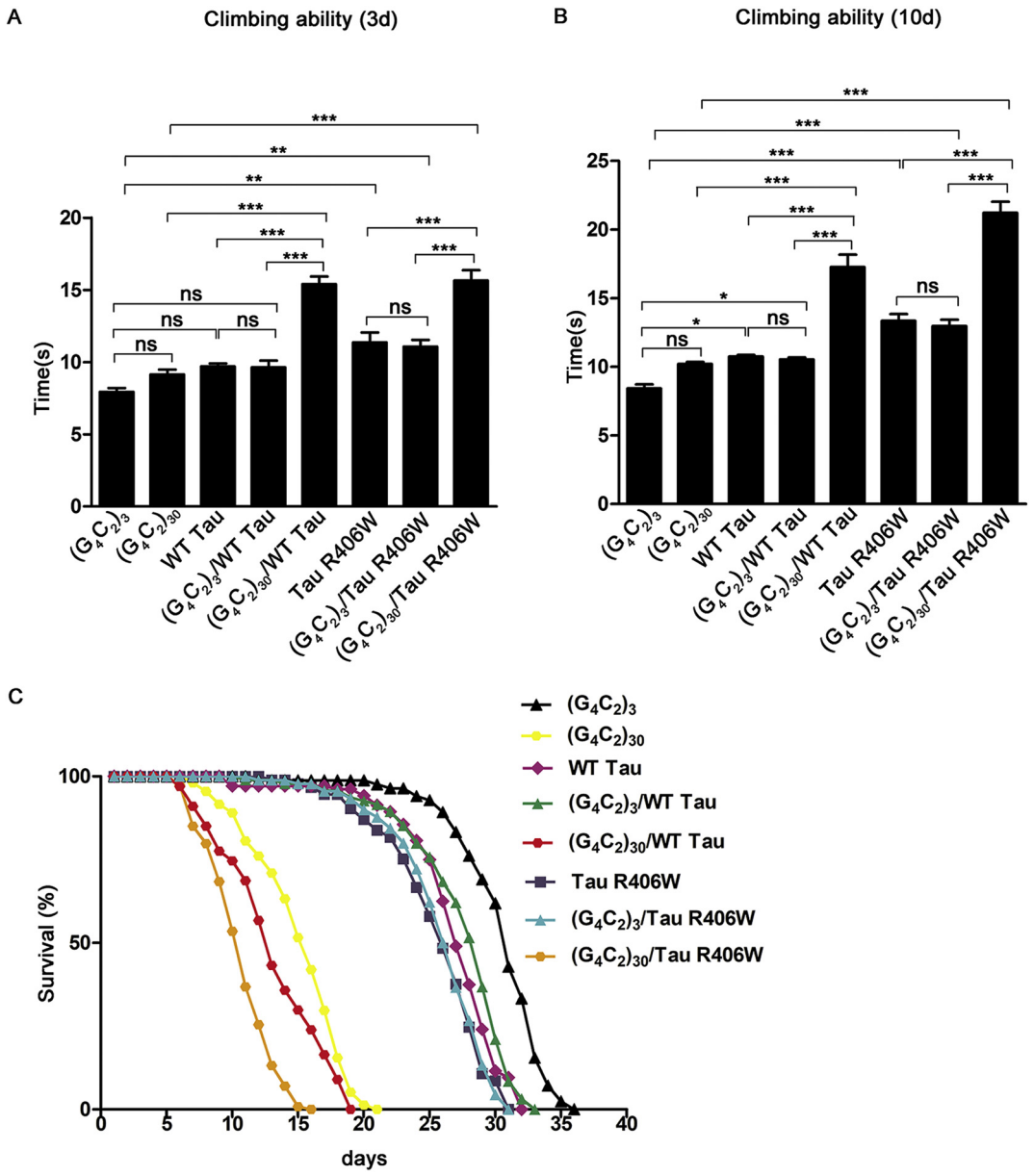

Fig. 2. Enhanced climbing defects and shortened lifespan in adult flies.

A. climbing ability (see Methods for details) of flies measured at 3 days. *p < 0.05; **p < 0.01; ***p < 0.001 after controlling for multiple testing using one-way ANOVA with the Tukey posthoc test.

B. climbing ability of flies measured at 10 days. *p < 0.05; **p < 0.01; ***p < 0.001 after controlling for multiple testing using one-way ANOVA with the Tukey posthoc test.

C. Flies co-expressing $(G_4C_2)_{30}$ and Tau (either WT or R406W) have a significantly shorter lifespan in comparison to other genotypes tested.

(*tub-Gal80ts*). The temperature sensitive Gal80 repressor under the control of the *tubulin* promoter can selectively control the binding affinity of Gal4 to the *UAS* sequence. We used the elav-Gal4;tub-Gal80^{ts} to study the consequences of $(G_4C_2)_{30}$ and Tau in adult neurons of the fly. Elav-Gal4;;tub-Gal80^{ts} females were crossed with +/y;$(G_4C_2)_{30}$/cyo; Tau/TM3 at 25 °C and offspring were maintained at 25 °C until eclosion, then male offspring (elav-GAL4/y; $(G_4C_2)_{30}$/+; tub-Gal80^{ts}/Tau) were collected and shifted immediately to a restrictive temperature of 29 °C. The $(G_4C_2)_{30}$ and Tau expression was activated as soon as the flies shifted to 29 °C. The flies were raised for 10 days or longer at 29 °C to perform the climbing assay, lifespan analysis and western blot (Zhang et al., 2015). Male flies were used because the phenotype is relatively uniform and stable compared to females which show a more heterogeneous phenotype.

2.2. Light microscopy and scanning electron microscopy

For light microscopy (LM) images, whole flies were analyzed with an OLYMPUS DP72 microscope. For scanning electron microscopy (SEM) images, whole flies were analyzed with an JEOL JSM-6360-LA scanning electron microscope.

2.3. Climbing assay

Climbing assays were performed as previously described (Park et al., 2006). Groups of ten 3-day-old or 10-day-old male flies were transferred into 1.25-cm diameter and 28-cm tall plastic tubes with 1 h incubation at room temperature to wake from anesthesia and acclimate to the new environment. Vials were then tapped until all flies were at the bottom, and then climbing time was scored. The arrival time of the

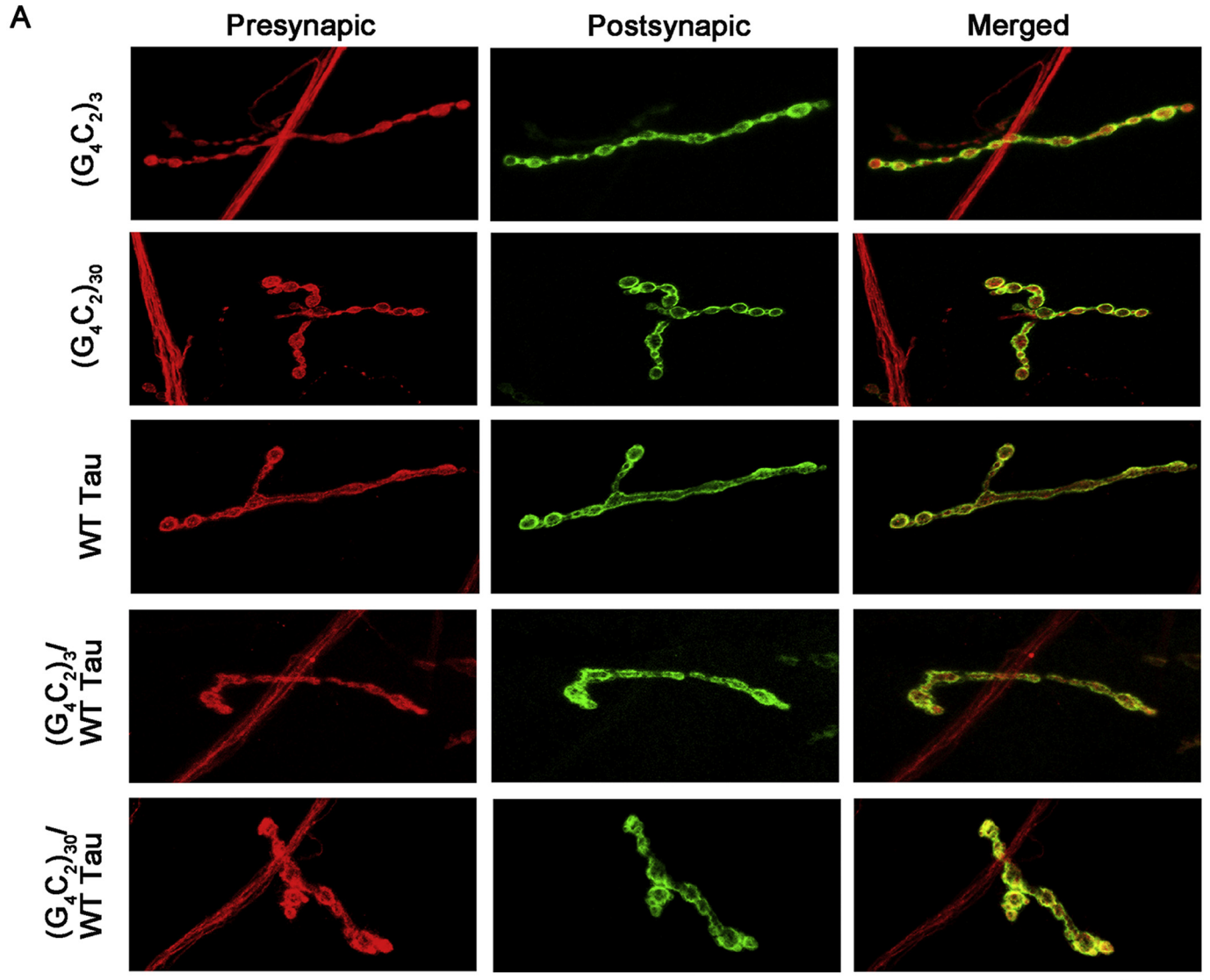

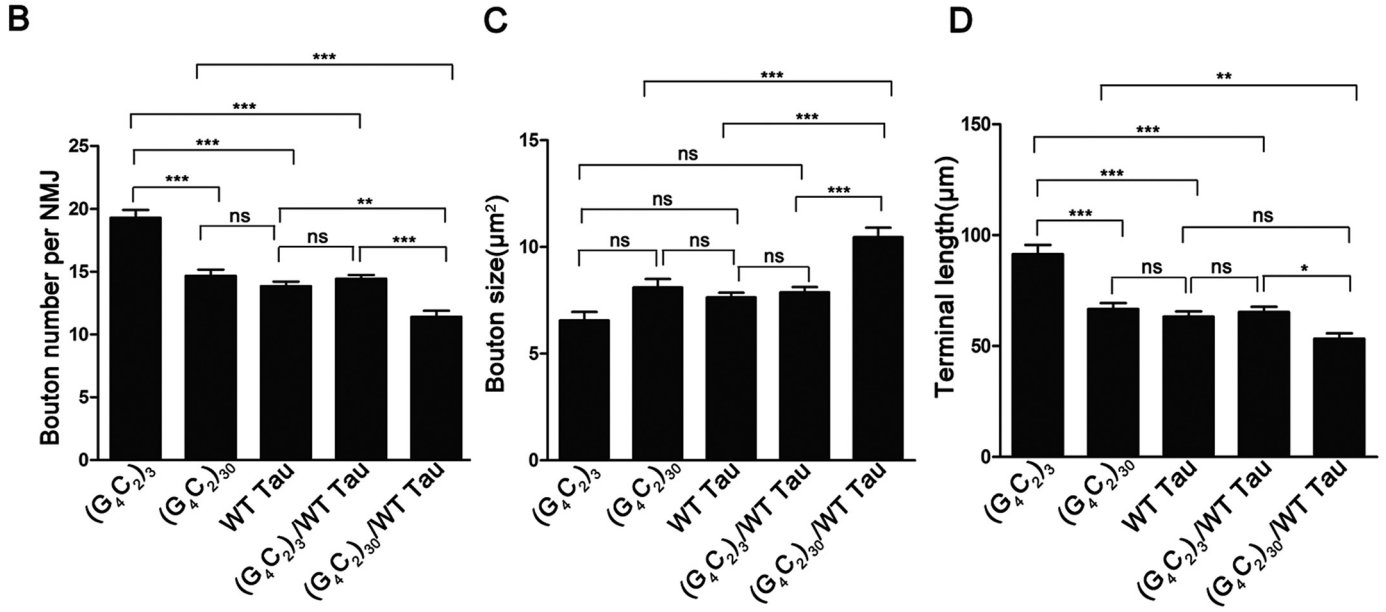

(caption on next page)

Fig. 3. NMJ morphological abnormalities caused by $(G_4C_2)_{30}$/WT Tau expression.
A. Staining of the type Ib bouton in muscle 4 in abdominal segments 3 and 4. HRP (red), stained presynaptic neuronal membranes; DLG (green) stained the postsynaptic muscle membrane surrounding each bouton.
B. Bouton number in larvae expressing G_4C_2 and Tau WT. *P < 0.05; **P < 0.01; ***P < 0.001 after controlling for multiple testing using one-way ANOVA with the Tukey posthoc test.
C. Bouton size in larvae expressing G_4C_2 and Tau WT. *P < 0.05; **P < 0.01; ***P < 0.001 after controlling for multiple testing using one-way ANOVA with the Tukey posthoc test.
D. Terminal length in larvae expressing G_4C_2 and Tau WT. *P < 0.05; **P < 0.01; ***P < 0.001 after controlling for multiple testing using one-way ANOVA with the Tukey posthoc test. (For interpretation of the references to colour in this figure legend, the reader is referred to the web version of this article.)

fifth fly at the 15-cm finish line was collected and analyzed. Three trials were repeated for each group. For each genotype, over 3 groups of male flies were examined, comparisons were made using one-way ANOVA with the Tukey posthoc test.

2.4. Lifespan analysis

For lifespan analysis, > 100 flies per genotype were collected in individual vials containing no > 30 flies and assayed for longevity as previously described (Wittmann et al., 2001). Flies were transferred to fresh vials every other day. Lifespan was measured by scoring dead flies remaining in the old vial and plotted using the Kaplan-Meir method. The median lifespan (MedLS) was calculated as the age when half of the flies had died, and the survival distribution of the two genotypic groups were compared using the log-rank (Mantel-Cox) test.

2.5. Larval NMJ staining

Third-instar larval muscles were dissected and stained using a modified protocol described by Dr. Wei Xie (Xing et al., 2014). In brief, wandering third instar larvae were dissected in PBS and fixed in 4% PFA for 20–25 min at room temperature. The samples were then incubated in the primary antibody solution (primary of the desired dilution +5% normal goat serum +0.2% PBST) overnight at 4 °C. To count type 1b synaptic bouton number, each genotype was double stained presynaptically with anti-HRP-Cy3 (1:200, Jackson Immunoresearch) and postsynaptically with anti-Disc large 1 (1:50, DSHB). The NMJs from muscle 4 of abdominal segments 2, 3, and 4 were imaged using a Leica TCS SP5 confocal station and ImageJ software (National Institutes of Health, Bethesda, MD, USA) to quantify the bouton numbers and sizes.

2.6. Protein preparation and Immunoblotting

To analyze the phosphorylation levels of Tau proteins, heads from adult *Drosophila* were homogenized in lysis buffer (10 mM Tris-HCl, 150 mM NaCl, 2% SDS, 10% glycerol, 1 mM PMSF, 1 × protein inhibitors cocktail, 1 × phosphatase inhibitors cocktail)). Protein extracts were mixed with SDS loading buffer and heated to 95 °C, and then centrifuged at 13,000*g* for 10 min before they were loaded onto a 10% SDS-PAGE gel. Primary antibodies include phospho-independent Tau antibody (anti-Total Tau; DAKO; 1:40000), phospho-dependent Tau antibodies: AT-8 (specific for the phosphoserine 202 epitope; Pierce; 1:400); AT-180 (specific for the phosphoserine 231 epitope; Pierce; 1:400), AT-270 (specific for the phosphothreonine 181 epitope; Pierce; 1:400), pCDK5 (Santa Cruz; sc-377,558; 1:400), and anti-β-actin antibody (mAbcam 8224;1 μg/mL). Secondary antibodies conjugated to HRP (SouthernBiotech) were used at a 1:10,000 dilution, and signal detection was performed with chemiluminescence (Pierce Biotechnology). All Western blots were repeated at least three times with similar results.

2.7. Extraction of soluble and insoluble tau proteins

Extraction of soluble and insoluble proteins were performed as described (Feuillette et al., 2010). Thirty adult fly heads were dissected and homogenized in 100 μL radio immunoprecipitation assay (RIPA) buffer (50 mM Tris–HCl,pH 8, 150 mM NaCl, 20 mM EDTA, 1% Nonidet-P40 (Calbio-chem, La Jolla, CA, USA) (*v*/v), 50 mM natrium fluoride, 20 mM N-ethylmaleimide, and a cocktail of protease inhibitors (Sigma-Aldrich)). Samples were placed under agitation at 4 °C for 1 h and then centrifuged at 11,300*g* for 20 min at 4 °C to remove cellular debris. The supernatant was collected as the RIPA fraction. The pellet was washed once in RIPA, then homogenized in 70 μL of 70% formic acid (FA) and centrifuged again at 11,300*g* for 20 min. The supernatant was collected, and, after evaporation of the formic acid by Speed Vac, the pellet was resuspended in 30 μL sodium dodecyl sulfate– polyacrylamide gel electrophoresis (SDS–PAGE) sample buffer (240 mM Tris–HCl, pH 6.8, 6% SDS, 30% glycerol, 0.06% bromophenol blue). The RIPA fraction contained soluble human Tau (h-Tau) and detergent-extractable insoluble h-Tau, and the FA fraction contained detergent-insoluble h-Tau that can be extracted with 70% formic acid. Twenty micrograms of protein from the RIPA fraction and 30 μL FA fractions were resolved by a 10% SDS–PAGE.

2.8. Immunostaining

Heads from adult flies at 7d post-eclosion were fixed in formalin, embedded in OCT compound and 10-μm cryostat sections were prepared. For immunostaining, primary antibody was AT8 (specific for the phosphoserine 202 epitope; Pierce; 1:50) and secondary antibody was Cy3-conjugated goat anti-mouse (1500; Jackson Labs). Nuclei were counterstained with DAPI (Sigma, D9542). Samples were viewed on a ZEISS confocal laser scanning microscope. Z stacks (merged images) were constructed from ten focal planes for each final image.

2.9. Statistical analysis

All statistical models were tested using Analysis of Variance (ANOVA), and differences between groups were determined using Tukey's Studentized Range Test to control for multiple testing.

3. Results

3.1. $(G_4C_2)_{30}$ enhances the toxic effect of tau in Drosophila eyes

In order to test the genetic association between G_4C_2 expansion and Tau, we expressed two different length G_4C_2 repeats in the *Drosophila* eye using the GMR-GAL4 driver. The first line contained three G_4C_2 repeats, and the second line had 30 G_4C_2 repeats. The G_4C_2 lines were crossed with two different Tau lines: a four C-terminal tandem repeats (4R) isoform of human wild-type (WT) Tau and an R406W mutant Tau. The R406W is a missense mutation associated with a familial form of FTD (Wittmann et al., 2001). Overexpression of WT Tau and Tau R406W caused a moderate eye degeneration phenotype: the eyes reduced in size and displayed a rough phenotype (Figure 1Ac and 1Ad, respectively; 1B). Expression of $(G_4C_2)_{30}$ alone showed cell death, loss of pigmentation, and ommatidial disruption (Figure 1Ab), but no significant difference in eye size was observed when compared to $(G_4C_2)_3$ flies (Fig. 1B). When the $(G_4C_2)_{30}$ construct was co-expressed with WT Tau or R406W, enhanced Tau toxicity was seen, resulting in smaller eyes, severely fused ommatidia, and pigmentation loss (Figure 1Ak

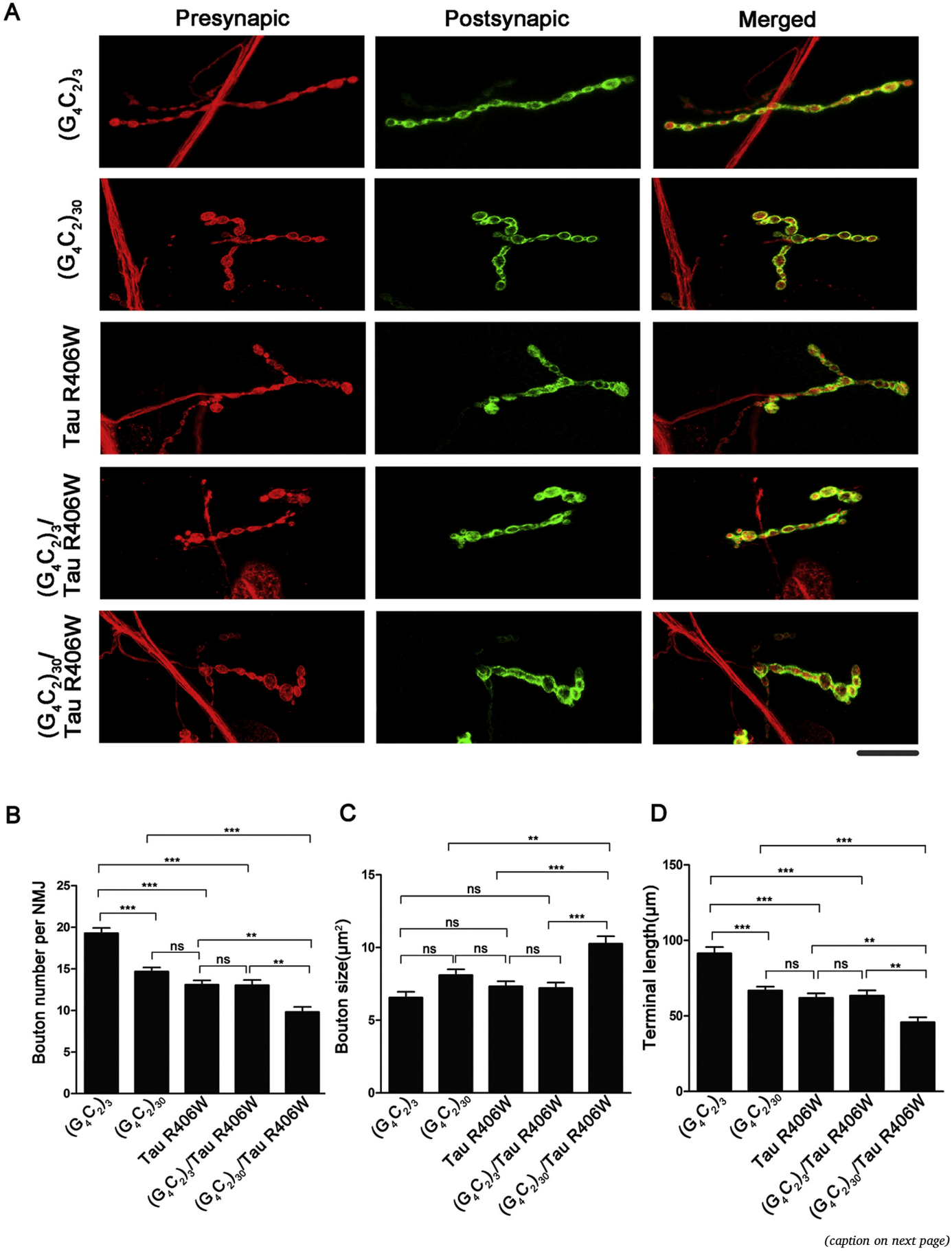

(caption on next page)

Fig. 4. NMJ morphological abnormalities caused by $(G_4C_2)_{30}$/Tau R406W expression.
A. Staining of the type Ib bouton in muscle 4 in abdominal segments 3 and 4. HRP (red), stained presynaptic neuronal membranes; DLG (green) stained the postsynaptic muscle membrane surrounding each bouton.
B. Bouton number in larvae expressing G_4C_2 and Tau R406W. *P < 0.05; **P < 0.01; ***P < 0.001 after controlling for multiple testing using one-way ANOVA with the Tukey posthoc test.
C. Bouton size in larvae expressing G_4C_2 and Tau R406W. *P < 0.05; **P < 0.01; ***P < 0.001 after controlling for multiple testing using one-way ANOVA with the Tukey posthoc test.
D. Terminal length in larvae expressing G_4C_2 and Tau R406W. *P < 0.05; **P < 0.01; ***P < 0.001 after controlling for multiple testing using one-way ANOVA with the Tukey posthoc test.

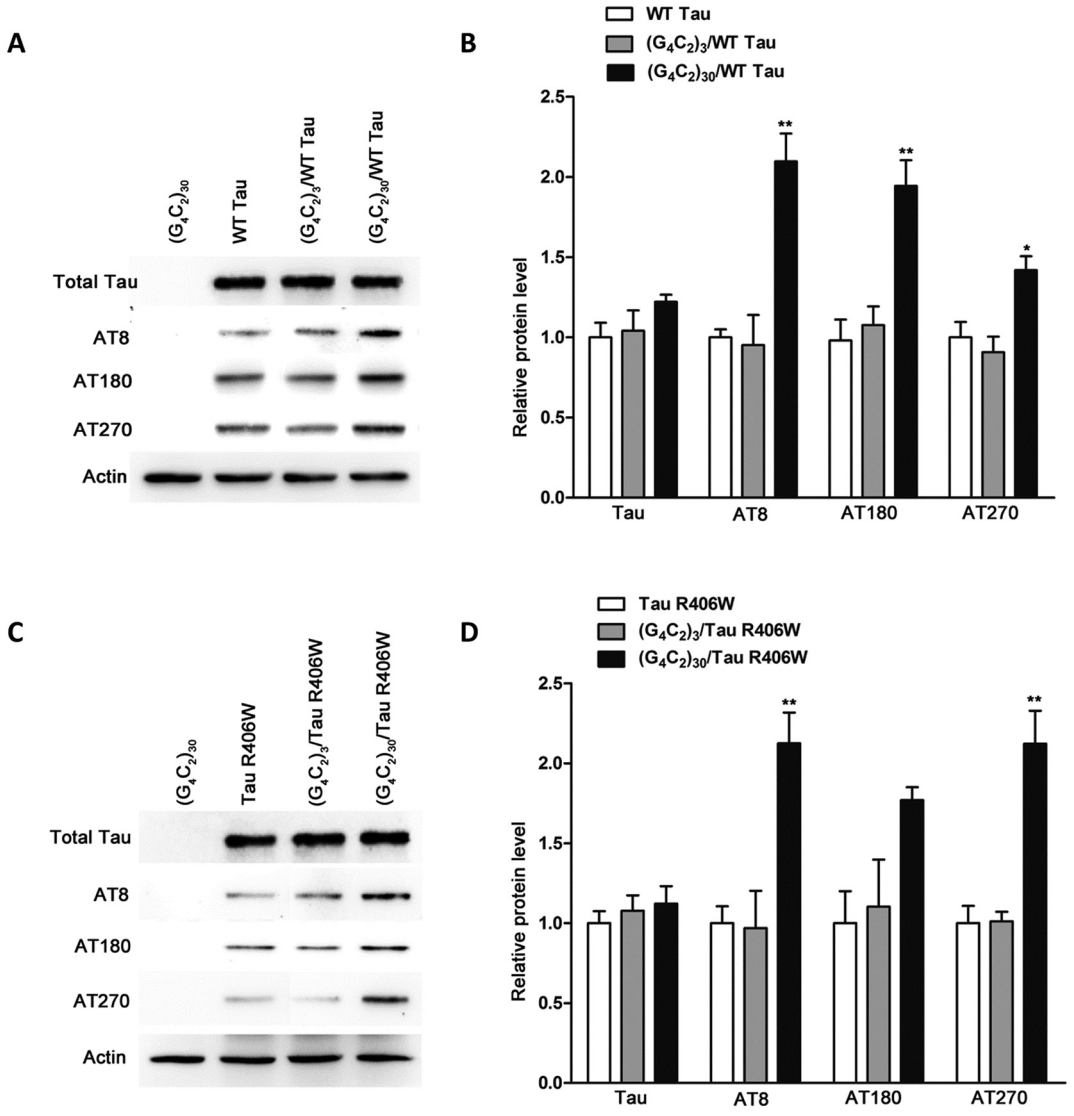

Fig. 5. Tau phosphorylation levels were increased by $(G_4C_2)_{30}$.
A, C. Western blot analyses comparing total Tau and Tau phosphorylation in Tau, $(G_4C_2)_3$/Tau and $(G_4C_2)_{30}$/Tau flies.
B, D. Bar graphs show quantitative analysis of relative phosphorylation level changes after $(G_4C_2)_{30}$ and Tau coexpression. ** significantly different from all other groups; * significantly different from $(G_4C_2)_3$/Tau line only.

and1Al, respectively; 1B). In contrast, co-expression of $(G_4C_2)_3$ and either form of Tau had no additional effect on Tau-induced retinal toxicity (Figure 1Ai vs. 1Ac and 1Aj vs. 1Ad, respectively). These results indicate that expression of the $(G_4C_2)_{30}$ repeat enhances the toxic effect of both wild-type and mutant forms of Tau.

3.2. $(G_4C_2)_{30}$ aggravates motor dysfunction in adult tau transgenic flies

Motor behavior has been used to interrogate neuronal function in various neurodegenerative models. The expression of $(G_4C_2)_{30}$ in all cells of the peripheral and central nervous system using elav-GAL4 caused lethality in early development. Therefore, we used the elav-GAL4/tub-Gal80^{ts} system to express the expanded G_4C_2 repeat and Tau in adult neurons. The crossed flies were raised at 25 °C until male offspring were collected and shifted to a restrictive temperature of 29 °C at the end of each experiment. Neuronal expression of $(G_4C_2)_{30}$ or Tau throughout adulthood caused moderate climb defects compared to $(G_4C_2)_3$ flies (Fig. 2A-B). However, flies expressing both $(G_4C_2)_{30}$ and Tau had an exacerbated movement impairment and reduced lifespan (Fig. 2). Co-expression of $(G_4C_2)_3$ and Tau (either WT or R406W) had

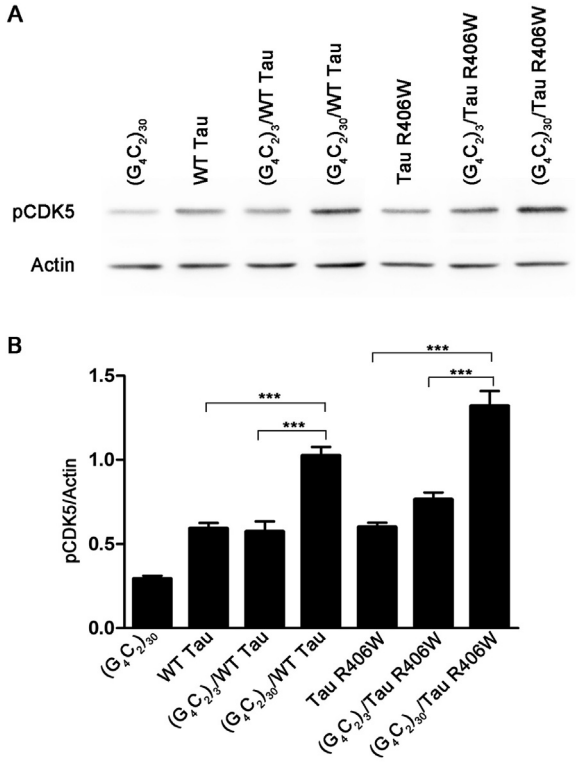

Fig. 6. $(G_4C_2)_{30}$ enhanced CDK5 kinase activity.
A. Western blot analyses of pCDK5 in 1-week-old flies expressing $(G_4C_2)_{30}$, Tau (WT or R406W), $(G_4C_2)_3$/Tau (WT or R406W) or $(G_4C_2)_{30}$/Tau (WT or R406W); B. Bar graphs show quantitative analysis of pCDK5 level changes after $(G_4C_2)_{30}$ and Tau coexpression. ***$p < .001$ after controlling for multiple testing using one-way ANOVA with the Tukey posthoc test.

no effect on Tau-induced movement impairment and lifespan. These results indicate that motor dysfunction could be aggravated by the co-expression of the expanded $(G_4C_2)_{30}$ repeat and Tau.

3.3. $(G_4C_2)_{30}$ exacerbates the NMJ morphological abnormalities caused by Tau in larval motor neurons

The impaired locomotion caused by overexpression of Tau in motor neurons suggests that a likely cause of this deficit could be abnormal functioning of the neuromuscular junction (NMJ) (Augustinack et al., 2002). Previous studies demonstrated that overexpression of human Tau (wild-type and R406W) or the G_4C_2 expansion in *Drosophila* motor neurons resulted in abnormal NMJ morphology features. The effects of the expanded G_4C_2 repeat with Tau on NMJ features has not been investigated. Therefore, we used the pan-neuronal driver elav-Gal4 to express G_4C_2 and Tau in neurons beginning at embryonic stages. There were significantly less boutons and shortened terminal length at the NMJ terminals when WT Tau and $(G_4C_2)_{30}$ were co-expressed compared with expression of either of them alone (Fig. 3A, B, D). Bouton size was also increased when both genes were expressed (Fig. 3A, C). Co-expression of $(G_4C_2)_3$ with WT Tau had no effect on bouton number, bouton size or terminal length compared with expression of WT Tau alone (Fig. 3A-D). The result for Tau R406W was similar (Fig. 4). These data together suggest that the NMJ defects were exacerbated when the $(G_4C_2)_{30}$ repeat and Tau were co-expressed in larval motor neurons.

3.4. Tau phosphorylation and solubility are altered by $(G_4C_2)_{30}$

Because the toxic effects of Tau in humans is closely related to its phosphorylation status, immunoblot analyses were used to detect the levels of AT8, AT180, and AT270, which are disease-associated phosphorylation sites in Tau-mediated neurotoxicity. Transgenic male flies overexpressing the G_4C_2 repeat expansion and Tau using the elav-Gal4/tub-Gal80^{ts} system were collected and aged for 1 week in 29 °C. After three independent experiments, a significant increase in AT8 and AT270 levels were observed in flies co-expressing $(G_4C_2)_{30}$ and Tau compared to Tau alone or the $(G_4C_2)_3$/Tau co-expression flies (Fig. 5). AT180 levels were significantly increased for $(G_4C_2)_{30}$/Tau WT flies, but the increased level of AT180 did not reach significance in $(G_4C_2)_{30}$/Tau R406W flies.

In humans, the proline directed protein kinase CDK5 is a good candidate for directly modulating tau phosphorylation. Aberrant CDK5 kinase activity results in Tau hyperphosphorylation causing neurofibrillary tangles (NFT), which is a hallmark of AD (Baumann et al., 1993; Pei et al., 1998). In order to determine whether CDK5 kinase activity was increased in $(G_4C_2)_{30}$/Tau flies, we detected pCDK5 level in 1-week flies using the elav-Gal4/tub-Gal80^{ts} system at 29 °C. After three independent experiments, a significant increase in pCDK5 levels was observed in flies co-expressing $(G_4C_2)_{30}$ and Tau (WT or R406W) compared to Tau alone or the $(G_4C_2)_3$/Tau co-expression (Fig. 6). These data suggested that the expression of $(G_4C_2)_{30}$ enhanced CDK5 kinase activity, leading to elevated Tau phosphorylation.

As in human Tauopathies, Tau hyperphosphorylation can induce intracellular aggregates of insoluble Tau protein. Analysis of insoluble Tau has provided a powerful tool to understand the development of Tau pathology (Julien et al., 2012). To determine whether expanded G_4C_2 repeats affect the quantity of insoluble Tau, a formic acid extraction method was applied. Head lysates from flies expressing the G_4C_2 repeat expansion and Tau were fractionated into soluble and insoluble materials, and the latter was extracted with 70% formic acid (FA) to probe for aggregates (Papanikolopoulou and Skoulakis, 2015). As shown in Fig. 7, a main band of 50–60 kDa was seen, corresponding to monomeric Tau proteins for the soluble RIPA fraction. Both Tau WT and Tau R406W flies showed increased levels in 1-week flies compared with 2-day flies without obvious difference between $(G_4C_2)_3$ and $(G_4C_2)_{30}$. For the insoluble fraction extracted with FA buffer, an elevated level of the insoluble monomeric Tau proteins was observed in $(G_4C_2)_{30}$/Tau WT flies compared to $(G_4C_2)_3$/Tau WT flies. Notably, both insoluble monomeric and high-molecular-weight (HMW) forms of Tau proteins were increased in $(G_4C_2)_{30}$/Tau R406W flies compared with $(G_4C_2)_3$/Tau R406W flies, particularly in the 1-week flies, indicating that expanded G_4C_2 repeats enhanced the aggregation of Tau R406W.

We then examined the retinal localization of Tau co-expressed with $(G_4C_2)_{30}$ using the monoclonal antibody AT8, which recognizes a phosphorylated epitope unique to Tau within paired helical filaments (PHF) (Matsuo et al., 1994). PHFs are a major component of the neurofibrillary tangles involved in the pathology of Alzheimer's disease. No staining for AT8 was observed in the $(G_4C_2)_{30}$ line, punctate aggregate staining was observed in $(G_4C_2)_3$/Tau WT transgenic eyes, while more heavily dotted aggregates were observed in the lamina and medulla of flies co-expressing $(G_4C_2)_{30}$ and Tau WT within photoreceptor neurons. Strikingly, abundant fibrillar- shaped aggregates were observed in $(G_4C_2)_{30}$/Tau R406W flies (Fig. 7C). The appearance of phospho-tau aggregates was enhanced when $(G_4C_2)_{30}$ was co-expressed. These data together suggested that Tau phosphorylation and aggregate formation were altered by expanded G_4C_2 repeats.

4. Discussion

Growing evidence has shown that the co-occurrence of multiple mutations could impact activity and toxicity, producing striking changes in disease progression (Pocas et al., 2015; Roy and Jackson, 2014). Here, we explored the relationship between the G_4C_2 repeat expansion in *C9ORF72* and Tau in *Drosophila*. We showed that coexpression of $(G_4C_2)_{30}$ and Tau can produce a synergistic deterioration, characterized by rough eyes, motor function, lifespan and NMJ morphology in *Drosophila*. Compared with the normal allele of $(G_4C_2)_3$

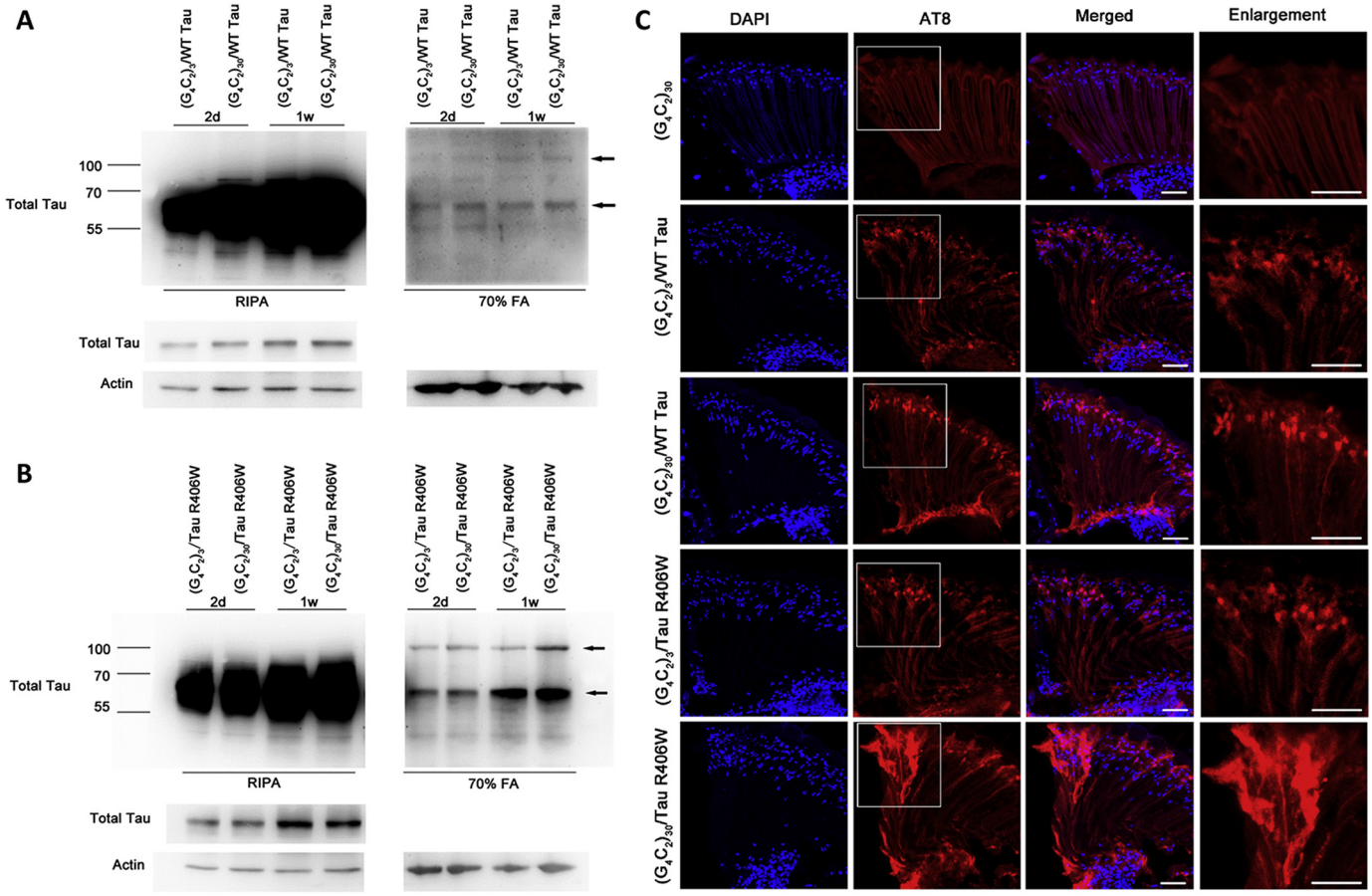

Fig. 7. Tau solubility status was altered by $(G_4C_2)_{30}$.

A, B. Proteins were extracted from fly heads with RIPA buffer and the insoluble fraction was solubilized in 70% FA and used for western blotting. A. Western blots of 2-day-old and 1-week-old flies expressing $(G_4C_2)_3$/Tau WT or $(G_4C_2)_{30}$/Tau WT; B. Western blots of 2-day-old and 1-week-old flies expressing $(G_4C_2)_3$/Tau R406W or $(G_4C_2)_{30}$/Tau R406W.

C. Confocal analysis of cryostat sections using an antibody recognizing phosphorylated PHF-Tau in the retina. Red: AT8+ Cy3-conjugated anti-mouse IgG, show aggregates of phosphorylated Tau with pan-neuronal expression in adult flies. Blue: DAPI, stained nuclei. Scale bar: 20 μm.

repeats, the $(G_4C_2)_{30}$ expansion increased Tau phosphorylation and promoted Tau R406W aggregation. This is the first demonstration to reveal the genetic interaction between G_4C_2 repeat expansion and Tau.

Tau hyperphosphorylation is considered to be highly associated with its toxicity in multiple neurodegenerative diseases (Spillantini and Goedert, 2013; Mann and Snowden, 2017). Although phosphorylation sites can be occupied in normal and Tauopathy samples, greater phosphorylation levels and an increased number of phosphorylation sites in the latter, have been seen in comparative analyses (Cooper-Knock et al., 2014; Alonso and Cohen, 2018). Sequential changes of Tau-site-specific phosphorylation has been studied during neurofibrillary development in AD brain samples: hyper-phosphorylation at AT8 (S199 + S202 + T205), AT180 (T231) and AT270 (T181) were found to be early events in NFT formation, indicative of the presence of pre-tangle Tau (Neddens et al., 2018; Kimura et al., 1996; Augustinack et al., 2002). We demonstrated that the $(G_4C_2)_{30}$ expansion is able to cause an increase in the levels of AT8, AT180 and AT270, suggesting that the G_4C_2 expansion can increase Tau phosphorylation. Tau phosphorylation is a critical driver in Tau protein accumulation and aggregation (Iqbal et al., 2016). We also detected that the $(G_4C_2)_{30}$ expansion increased the aggregation of R406W mutant Tau; however, no obvious aggregation was found with wild-type Tau, potentially because the R406W mutation changes the conformation of Tau, making it a better substrate for aggregation. Previous research also found that fewer moles of phosphate per mole of protein were required for filament formation in the Tau mutant proteins (Alonso and Cohen, 2018).

Another important question is how the $(G_4C_2)_{30}$ repeat expansion could affect Tau phosphorylation. It was reported that Tau was phosphorylated at many sites via several protein kinases, in particular, phosphorylation at Ser/Thr residues in proline-rich domains has been seen. These residues are targeted by proline-directed protein kinases such as extracellular signal-regulated kinase (ERK), glycogen synthase kinase 3β (GSK3β), and cyclin-dependent kinase-5 (CDK5) (Iqbal et al., 2016). CDK5 has attracted attention because it is the primer for other phosphorylation sites. For example, CDK5 primes Tau by phosphorylating Ser235, leading to subsequent Thr231 phosphorylation by GSK3β. Studies indicate that CDK5 is the primer for a series of ordered phosphorylation, including Ser235, Thr231, Ser404, Ser396, Ser199, Ser202, and Thr205, which are sites that are hyperphosphorylated in AD brains (Castro-Alvarez et al., 2014). A recent report showed that expression of expanded G_4C_2 repeats caused neuronal cell toxicity in Neuro-2a cells, and enhanced the activity of CDK5, but the protein level was not changed (Shen et al., 2018). In our study, pCDK5 level was increased in $(G_4C_2)_{30}$/Tau (WT or R406W) flies when compared with in $(G_4C_2)_3$/Tau (WT or R406W) flies, indicating that the elevated Tau phosphorylation may be regulated by $(G_4C_2)_{30}$ through enhanced CDK5 activity. Recent studies have indicated that the pathogenesis of the G_4C_2 expansion is caused by the expression of dipeptide proteins that are expressed via repeat-associated non-ATG initiated (RAN) translation (Mizielinska et al., 2014; Moens et al., 2018). The exact mechanism of how $(G_4C_2)_{30}$ may affect Tau phosphorylation needs to be further elucidated.

In summary, we have demonstrated the genetic interaction between the G_4C_2 repeat expansion and the Tau toxicity for both WT and mutant Tau, and we have shown that the expanded G_4C_2 repeat could increase Tau phosphorylation level and promote Tau R406W aggregation. These results suggest a possible link between G_4C_2 repeat expansion and Tau toxicity, and provide novel insights into the neuronal toxicity associated with expanded G_4C_2 repeat expansion and Tau.

Acknowledgements

This study was supported by the National Natural Science Foundation of China (81571253 and 81771385) and the Hunan Provincial Natural Science Foundation of China (2016JJ3135).

Conflict of interest

The authors declare that they have no conflict of interest.

References

Alonso, A.D., Cohen, L.S., 2018. Our Tau tales from normal to pathological behavior. J. Alzheimers Dis. 64 (s1), S507–S516.
Augustinack, J.C., Schneider, A., Mandelkow, E.M., Hyman, B.T., 2002. Specific tau phosphorylation sites correlate with severity of neuronal cytopathology in Alzheimer's disease. Acta Neuropathol. 103 (1), 26–35.
Baumann, K., Mandelkow, E.M., Biernat, J., Piwnica-Worms, H., Mandelkow, E., 1993. Abnormal Alzheimer-like phosphorylation of tau-protein by cyclin-dependent kinases cdk2 and cdk5. FEBS Lett. 336 (3), 417–424.
Bieniek, K.F., Murray, M.E., Rutherford, N.J., Castanedes-Casey, M., DeJesus-Hernandez, M., Liesinger, A.M., Baker, M.C., Boylan, K.B., Rademakers, R., Dickson, D.W., 2013. Tau pathology in frontotemporal lobar degeneration with C9ORF72 hexanucleotide repeat expansion. Acta Neuropathol. 125 (2), 289–302.
van Blitterswijk, M., Baker, M.C., DeJesus-Hernandez, M., Ghidoni, R., Benussi, L., Finger, E., Hsiung, G.Y., Kelley, B.J., Murray, M.E., Rutherford, N.J., et al., 2013. C9ORF72 repeat expansions in cases with previously identified pathogenic mutations. Neurology 81 (15), 1332–1341.
Bonini, N.M., Fortini, M.E., 2003. Human neurodegenerative disease modeling using Drosophila. Annu. Rev. Neurosci. 26, 627–656.
Castro-Alvarez, J.F., Uribe-Arias, S.A., Mejia-Raigosa, D., Cardona-Gomez, G.P., 2014. Cyclin-dependent kinase 5, a node protein in diminished tauopathy: a systems biology approach. Front. Aging Neurosci. 6, 232.
Chan, H.Y., Bonini, N.M., 2000. Drosophila models of human neurodegenerative disease. Cell Death Differ. 7 (11), 1075–1080.
Cooper-Knock, J., Shaw, P.J., Kirby, J., 2014. The widening spectrum of C9ORF72-related disease; genotype/phenotype correlations and potential modifiers of clinical phenotype. Acta Neuropathol. 127 (3), 333–345.
DeJesus-Hernandez, M., Mackenzie, I.R., Boeve, B.F., Boxer, A.L., Baker, M., Rutherford, N.J., Nicholson, A.M., Finch, N.A., Flynn, H., Adamson, J., et al., 2011. Expanded GGGGCC hexanucleotide repeat in noncoding region of C9ORF72 causes chromosome 9p-linked FTD and ALS. Neuron 72 (2), 245–256.
Elahi, F.M., Miller, B.L., 2017. A clinicopathological approach to the diagnosis of dementia. Nat. Rev. Neurol. 13 (8), 457–476.
Ferrari, R., Mok, K., Moreno, J.H., Cosentino, S., Goldman, J., Pietrini, P., Mayeux, R., Tierney, M.C., Kapogiannis, D., Jicha, G.A., et al., 2012. Screening for C9ORF72 repeat expansion in FTLD. Neurobiol. Aging 33 (8), 1850 e1851–1811.
Feuillette, S., Miguel, L., Frebourg, T., Campion, D., Lecourtois, M., 2010. Drosophila models of human tauopathies indicate that Tau protein toxicity in vivo is mediated by soluble cytosolic phosphorylated forms of the protein. J. Neurochem. 113 (4), 895–903.
Gan, L., Cookson, M.R., Petrucelli, L., La Spada, A.R., 2018. Converging pathways in neurodegeneration, from genetics to mechanisms. Nat. Neurosci. 21 (10), 1300–1309.
Holtzman, D.M., Carrillo, M.C., Hendrix, J.A., Bain, L.J., Catafau, A.M., Gault, L.M., Goedert, M., Mandelkow, E., Mandelkow, E.M., Miller, D.S., et al., 2016. Tau: from research to clinical development. Alzheimers Dement. 12 (10), 1033–1039.
Hutton, M., Lendon, C.L., Rizzu, P., Baker, M., Froelich, S., Houlden, H., Pickering-Brown, S., Chakraverty, S., Isaacs, A., Grover, A., et al., 1998. Association of missense and 5′-splice-site mutations in tau with the inherited dementia FTDP-17. Nature 393 (6686), 702–705.
Iqbal, K., Liu, F., Gong, C.X., 2016. Tau and neurodegenerative disease: the story so far. Nat. Rev. Neurol. 12 (1), 15–27.
Julien, C., Bretteville, A., Planel, E., 2012. Biochemical isolation of insoluble tau in transgenic mouse models of tauopathies. Methods Mol. Biol. 849, 473–491.
Kimura, T., Ono, T., Takamatsu, J., Yamamoto, H., Ikegami, K., Kondo, A., Hasegawa, M., Ihara, Y., Miyamoto, E., Miyakawa, T., 1996. Sequential changes of tau-site-specific phosphorylation during development of paired helical filaments. Dementia 7 (4), 177–181.
Kimura, T., Sharma, G., Ishiguro, K., Hisanaga, S.I., 2018. Phospho-tau Bar code: analysis of phosphoisotypes of tau and its application to tauopathy. Front. Neurosci. 12, 44.
King, A., Al-Sarraj, S., Troakes, C., Smith, B.N., Maekawa, S., Iovino, M., Spillantini, M.G., Shaw, C.E., 2013. Mixed tau, TDP-43 and p62 pathology in FTLD associated with a C9ORF72 repeat expansion and p.Ala239Thr MAPT (tau) variant. Acta Neuropathol. 125 (2), 303–310.
Liu, Y., Yu, J.T., Zong, Y., Zhou, J., Tan, L., 2014. C9ORF72 mutations in neurodegenerative diseases. Mol. Neurobiol. 49 (1), 386–398.
Mann, D.M.A., Snowden, J.S., 2017. Frontotemporal lobar degeneration: pathogenesis, pathology and pathways to phenotype. Brain Pathol. 27 (6), 723–736.
Matsuo, E.S., Shin, R.W., Billingsley, M.L., Van deVoorde, A., O'Connor, M., Trojanowski, J.Q., Lee, V.M., 1994. Biopsy-derived adult human brain tau is phosphorylated at many of the same sites as Alzheimer's disease paired helical filament tau. Neuron 13 (4), 989–1002.
Mizielinska, S., Gronke, S., Niccoli, T., Ridler, C.E., Clayton, E.L., Devoy, A., Moens, T., Norona, F.E., Woollacott, I.O.C., Pietrzyk, J., et al., 2014. C9orf72 repeat expansions cause neurodegeneration in Drosophila through arginine-rich proteins. Science 345 (6201), 1192–1194.
Moens, T.G., Mizielinska, S., Niccoli, T., Mitchell, J.S., Thoeng, A., Ridler, C.E., Gronke, S., Esser, J., Heslegrave, A., Zetterberg, H., et al., 2018. Sense and antisense RNA are not toxic in Drosophila models of C9orf72-associated ALS/FTD. Acta Neuropathol. 135 (3), 445–457.
Murray, M.E., DeJesus-Hernandez, M., Rutherford, N.J., Baker, M., Duara, R., Graff-Radford, N.R., Wszolek, Z.K., Ferman, T.J., Josephs, K.A., Boylan, K.B., et al., 2011. Clinical and neuropathologic heterogeneity of c9FTD/ALS associated with hexanucleotide repeat expansion in C9ORF72. Acta Neuropathol. 122 (6), 673–690.
Neddens, J., Temmel, M., Flunkert, S., Kerschbaumer, B., Hoeller, C., Loeffler, T., Niederkofler, V., Daum, G., Attems, J., Hutter-Paier, B., 2018. Phosphorylation of different tau sites during progression of Alzheimer's disease. Acta Neuropathol Commun 6 (1), 52.
Papanikolopoulou, K., Skoulakis, E.M., 2015. Temporally distinct phosphorylations differentiate Tau-dependent learning deficits and premature mortality in Drosophila. Hum. Mol. Genet. 24 (7), 2065–2077.
Park, J., Lee, S.B., Lee, S., Kim, Y., Song, S., Kim, S., Bae, E., Kim, J., Shong, M., Kim, J.M., et al., 2006. Mitochondrial dysfunction in Drosophila PINK1 mutants is complemented by parkin. Nature 441 (7097), 1157–1161.
Pei, J.J., Grundke-Iqbal, I., Iqbal, K., Bogdanovic, N., Winblad, B., Cowburn, R.F., 1998. Accumulation of cyclin-dependent kinase 5 (cdk5) in neurons with early stages of Alzheimer's disease neurofibrillary degeneration. Brain Res. 797 (2), 267–277.
Pocas, G.M., Branco-Santos, J., Herrera, F., Outeiro, T.F., 2015. Domingos PM: alpha-Synuclein modifies mutant huntingtin aggregation and neurotoxicity in Drosophila. Hum. Mol. Genet. 24 (7), 1898–1907.
Poorkaj, P., Bird, T.D., Wijsman, E., Nemens, E., Garruto, R.M., Anderson, L., Andreadis, A., Wiederholt, W.C., Raskind, M., Schellenberg, G.D., 1998. Tau is a candidate gene for chromosome 17 frontotemporal dementia. Ann. Neurol. 43 (6), 815–825.
Rademakers, R., Neumann, M., Mackenzie, I.R., 2012. Advances in understanding the molecular basis of frontotemporal dementia. Nat. Rev. Neurol. 8 (8), 423–434.
Renton, A.E., Majounie, E., Waite, A., Simon-Sanchez, J., Rollinson, S., Gibbs, J.R., Schymick, J.C., Laaksovirta, H., van Swieten, J.C., Myllykangas, L., et al., 2011. A hexanucleotide repeat expansion in C9ORF72 is the cause of chromosome 9p21-linked ALS-FTD. Neuron 72 (2), 257–268.
Roy, B., Jackson, G.R., 2014. Interactions between tau and alpha-synuclein augment neurotoxicity in a Drosophila model of Parkinson's disease. Hum. Mol. Genet. 23 (11), 3008–3023.
Shen, J., Zhang, Y., Zhao, S., Mao, H., Wang, Z., Li, H., Xu, Z., 2018. Puralpha repaired expanded hexanucleotide GGGGCC repeat noncoding RNA-caused neuronal toxicity in neuro-2a cells. Neurotox. Res. 33 (4), 693–701.
Spillantini, M.G., Goedert, M., 2013. Tau pathology and neurodegeneration. Lancet Neurol. 12 (6), 609–622.
Spillantini, M.G., Murrell, J.R., Goedert, M., Farlow, M.R., Klug, A., Ghetti, B., 1998. Mutation in the tau gene in familial multiple system tauopathy with presenile dementia. Proc. Natl. Acad. Sci. U. S. A. 95 (13), 7737–7741.
Wang, Y., Mandelkow, E., 2016. Tau in physiology and pathology. Nat. Rev. Neurosci. 17 (1), 5–21.
Wittmann, C.W., Wszolek, M.F., Shulman, J.M., Salvaterra, P.M., Lewis, J., Hutton, M., Feany, M.B., 2001. Tauopathy in Drosophila: neurodegeneration without neurofibrillary tangles. Science 293 (5530), 711–714.
Xing, G., Gan, G., Chen, D., Sun, M., Yi, J., Lv, H., Han, J., Xie, W., 2014. Drosophila neuroligin3 regulates neuromuscular junction development and synaptic differentiation. J. Biol. Chem. 289 (46), 31867–31877.
Xu, Z., Poidevin, M., Li, X., Li, Y., Shu, L., Nelson, D.L., Li, H., Hales, C.M., Gearing, M., Wingo, T.S., et al., 2013. Expanded GGGGCC repeat RNA associated with amyotrophic lateral sclerosis and frontotemporal dementia causes neurodegeneration. Proc. Natl. Acad. Sci. U. S. A. 110 (19), 7778–7783.
Zhang, K., Donnelly, C.J., Haeusler, A.R., Grima, J.C., Machamer, J.B., Steinwald, P., Daley, E.L., Miller, S.J., Cunningham, K.M., Vidensky, S., et al., 2015. The C9orf72 repeat expansion disrupts nucleocytoplasmic transport. Nature 525 (7567), 56–61.